

# The brinker repressor system regulates injury-induced nociceptive sensitization in *Drosophila melanogaster*

Molecular Pain  
Volume 17: 1–10  
© The Author(s) 2021  
Article reuse guidelines:  
sagepub.com/journals-permissions  
DOI: 10.1177/17448069211037401  
journals.sagepub.com/home/mpx



Aidan McParland<sup>1,2,\*</sup>, Julie Moulton<sup>1,\*</sup>, Courtney Brann<sup>1,3</sup>,  
Christine Hale<sup>1,4</sup>, Yvonne Otis<sup>1</sup>, and Geoffrey Ganter<sup>1,5</sup> 

## Abstract

Chronic pain is a debilitating condition affecting millions of people worldwide, and an improved understanding of the pathophysiology of chronic pain is urgently needed. Nociceptors are the sensory neurons that alert the nervous system to potentially harmful stimuli such as mechanical pressure or noxious thermal temperature. When an injury occurs, the nociceptive threshold for pain is reduced and an increased pain signal is produced. This process is called nociceptive sensitization. This sensitization normally subsides after the injury is healed. However, dysregulation can occur which results in sensitization that persists after the injury has healed. This process is thought to perpetuate chronic pain. The Hedgehog (Hh) signaling pathway has been previously implicated in nociceptive sensitization in response to injury in *Drosophila melanogaster*. Downstream of Hh signaling, the Bone Morphogenetic Protein (BMP) pathway has also been shown to be necessary for this process. Here, we describe a role for nuclear components of BMP's signaling pathway in the formation of injury-induced nociceptive sensitization. Brinker (Brk), and Schnurri (Shn) were suppressed in nociceptors using an RNA-interference (RNAi) “knockdown” approach. Knockdown of Brk resulted in hypersensitivity in the absence of injury, indicating that it normally acts to suppress nociceptive sensitivity. Animals in which transcriptional activator Shn was knocked down in nociceptors failed to develop normal allodynia after ultraviolet irradiation injury, indicating that Shn normally acts to promote hypersensitivity after injury. These results indicate that Brk-related transcription regulators play a crucial role in the formation of nociceptive sensitization and may therefore represent valuable new targets for pain-relieving medications.

## Keywords

Nociceptor, hypersensitivity, injury, repressor, activator, ultraviolet, RNAi, pain

Date Received: 31 December 2020; Revised 7 July 2021; accepted: 16 July 2021

## Introduction

Pain is an essential sensation that alerts us to potential tissue damage. If injury occurs, the process of nociceptive sensitization acts to reduce further tissue damage while the wound heals. Nociceptive sensitization occurs as a result of cytokine-mediated communication to the nervous system from injured tissues and causes an increased behavioral response to normally innocuous stimuli (allodynia) and/or to noxious stimuli (hyperalgesia). Ideally, hypersensitivity would only manifest until the injured tissue is healed. However, in some cases it persists even after healing has occurred, resulting in the formation of various chronic pain states.

<sup>1</sup> College of Arts and Sciences, University of New England, Biddeford, ME, USA

<sup>2</sup> University of British Columbia, Vancouver, British Columbia, Canada

<sup>3</sup> College of Osteopathic Medicine, University of New England, Biddeford, ME, USA

<sup>4</sup> Graduate School of Biomedical Sciences and Engineering, University of Maine, Orono, ME, USA

<sup>5</sup> Center for Excellence in the Neurosciences, University of New England, Biddeford, ME, USA

\*The first two authors contributed equally to this work.

### Corresponding Author:

Geoffrey Ganter, College of Arts and Sciences, University of New England, Biddeford, ME, USA.

Email: gganter@une.edu



A 2016 study revealed that approximately 20% of the US adult population (50 million individuals) experienced chronic pain.<sup>1</sup> Globally, the prevalence of chronic pain is approximately 20% with 10% newly diagnosed on an annual basis.<sup>2</sup> The management of chronic pain is challenging and multifactorial. Clinically, chronic pain treatment modalities include behavioral modifications, opioid regimens, and anti-inflammatory mediated approaches, yet in many ways these therapeutics fail to directly target the root of the nociceptive hypersensitivity response. For decades, we have relied on opioid analgesics as a mainstay of therapy, despite their myriad of side-effects including significant potential for addiction. In 2017 alone, there were over 58 opioid prescriptions written for every 100 US citizens.<sup>3</sup> Between the years of 1999 and 2018 there was a 400% increase in prescription-related opioid related overdose deaths.<sup>4</sup> While we have made tremendous de-prescribing efforts within both the U.S. and globally, these alarming statistics demonstrate a need for alternative management strategies and improved understanding of the pathophysiology of chronic pain.

Nociceptive sensitization underlies chronic and neuropathic pain states at the cellular level, yet the mechanisms of this response have yet to be fully elucidated. A better understanding of the exact cellular mechanisms underlying nociceptive sensitization is likely to contribute to more targeted chronic pain management strategies.

*Drosophila melanogaster* represents a model that provides both substantial genetic similarity to humans, as well as a simplified platform and powerful genetic tools with which to explore the genetic underpinnings of disease. Previous studies have established an effective paradigm for studying nociceptive sensitization in *Drosophila* larvae, using ultraviolet (UV) induced injury to sensitize the primary nociceptive neurons, referred to here as nociceptors.<sup>5</sup> Nociceptors detect thermal stimuli using thermosensitive ion channels such as Transient Receptor Potential (TRP) channels Painless and dTRPA1.<sup>6–8</sup> After exposure to a defined UV dose, injured larvae exhibit heightened behavioral responses to both sub-noxious and noxious stimuli, suggesting that this model serves to effectively investigate both allodynia and hyperalgesia. Using this model, previous studies have demonstrated the necessity of Tumor Necrosis Factor alpha (TNF- $\alpha$ ),<sup>5</sup> Hedgehog (Hh),<sup>9</sup> Tachykinin (Tk),<sup>10</sup> and Bone Morphogenetic Protein (BMP)<sup>11–13</sup> signaling in the formation of nociceptive sensitization in response to UV induced injury. Epistasis experiments have suggested that these signaling pathways regulate TRP channels to modulate nociceptor sensitivity.<sup>9</sup>

Morphogens found in the Tk and Hh signaling pathways have been implicated in many developmental processes, ranging from larval body segment development,

to axon guidance and proliferation.<sup>14–20</sup> One extensively studied factor downstream of the Hh signaling pathway is Decapentaplegic (Dpp), a functional homolog of mammalian BMP 2/4 and a member of the TGF- $\beta$  (Transforming Growth Factor Beta) superfamily of signaling proteins.<sup>21–23</sup> In *Drosophila*, Dpp is known to act as a graded morphogen and drives the development of stem cells, imaginal discs, and organizes dorsoventral symmetry.<sup>14</sup> TGF- $\beta$  signaling in general, and specifically Dpp signaling operates through activation of a tetrameric enzyme-linked receptor complex, leading to the phosphorylation of intracellular signaling molecule Mothers Against Decapentaplegic (Mad), which, with Medea (Med), then translocates to the nucleus.<sup>24</sup> Previous work has revealed the necessity of Dpp, its receptors, and the signal transducers Mad and Med<sup>11</sup> in the formation of injury-induced behavioral hypersensitivity, suggesting that the nociceptive sensitization response to injury likely occurs through transcriptional regulation (Figure 1).

Dpp's signal transducers Mad and Med exert their effects by activating transcription directly or by relieving the constitutive repression of the pathway's target genes

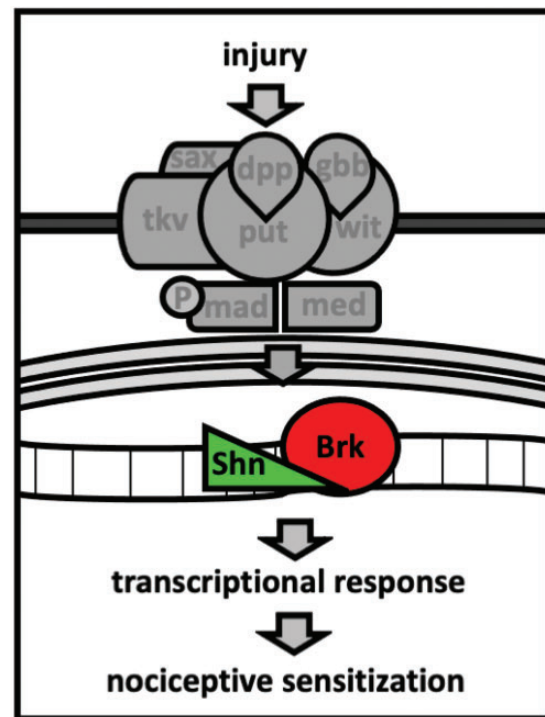


**Figure 1.** Schematic of injury-induced nociceptor sensitization via the Bone Morphogenetic Protein (BMP) Pathway. Injury by ultraviolet light activates the BMP signaling pathway including ligands, receptors, transducers, other mediators and, as demonstrated by the described experiments, the transcriptional repressor Brinker (Brk) and recruited activator Schnurri (Shn). In response, transcription of effector genes is regulated to sensitize the nociceptor and thereby promote healing.

by the transcriptional repressor Brk.<sup>24,25</sup> The Mad/Med complex is thought to recruit transcription regulator Shn that binds DNA and relieves Brk repression.<sup>26,27</sup> It is hypothesized, then, that since knockdown of Dpp produces failure to sensitize after injury,<sup>11</sup> knockdown of Shn may have the same effect, and knockdown of Brk may have an opposite effect, that is, hypersensitivity in the absence of injury.

In this study, tissue-specific RNAi-mediated suppression or “knockdown” was employed to establish a role for the transcriptional regulators Brk and Shn in the formation of nociceptive sensitization. Knockdown of Brk in nociceptors was found to be sufficient to produce behavioral hypersensitivity in the absence of tissue injury, while knockdown of Shn resulted in animals that were unable to form injury-induced allodynia. Although a direct mammalian homolog of Brk has yet to be identified, Shn resembles human HIV-EP1.<sup>28</sup> Indeed, most members of the BMP pathway show strong structural and functional conservation, in the case of Dpp so strongly that insect and mammal gene sequences may be substituted,<sup>29,30</sup> so it may be predicted that BMP-related repressors like Brk still await discovery in mammals. Elucidation of these mechanisms acting in the nuclei of the nociceptors themselves may contribute to a more thorough description of the processes underlying chronic pain in humans.

## Materials and methods

### Fly stocks and genetics

Fly stocks were maintained at 25°C unless otherwise indicated, in a 12 h light: 12 h dark cycle throughout the duration of the experiments. All genotypes were reared on standard cornmeal-yeast-sucrose diet. The GAL4/UAS system was used to drive the expression of RNA-interference transgenes in the larvae in nociceptive neurons. The driver used was ppk1.9-Gal4,<sup>5</sup> in which Gal4 is expressed in the pattern of the promoter of the pickpocket (ppk) gene, which is expressed nearly exclusively in the nociceptors.<sup>31,32</sup> UAS-inverted repeat lines were obtained from the Bloomington *Drosophila* Stock Center (BDSC) at Indiana University: *UAS-Brk<sup>IR-1</sup>* (BDSC#51789), *UAS-Brk<sup>IR-2</sup>* (BDSC#37493), *UAS-Shn<sup>IR-1</sup>* (BDSC#34689), *UAS-Shn<sup>IR-2</sup>* (BDSC#82982). A ppk1.9-Gal4, UAS-mCD8-GFP line was used to visualize nociceptors in immunohistochemistry experiments (Figure 2). A ppk1.9-CD4-tdTomato (BDSC#35844) was used to visualize nociceptors in the Shn::GFP experiment. A pBAC{shn-GFP.FBTB} line (BDSC#42671)<sup>33</sup> was used to observe GFP-tagged Shn (SHN::GFP) in nociceptor somata. Each GAL4/UAS experimental genotype was compared with two controls, one being the progeny of the *Gal4* driver crossed with a line

representing the genetic background of the *UAS* line, either *w<sup>1118</sup>* or *y<sup>1</sup>v<sup>1</sup>* (no UAS control). The other control consisted of the progeny of the *UAS* responder line crossed with *w<sup>1118</sup>* (no Gal4 control). In all experiments, large foraging third instar larvae were selected for analysis.

### UV exposure

Ultraviolet (UV) irradiation was used to induce tissue damage<sup>5</sup> in 3rd instar larvae. Larvae were washed with water and anesthetized with diethyl ether. Anesthetized larvae were then placed dorsal side up (approximately 20–30 larvae), on a microscope slide using two-sided tape and subjected to 12–18 (mJ/cm<sup>2</sup>) of UV-C irradiation using a Spectronics Corporation Spectrolinker XL-1000 ultraviolet crosslinker. UV dosage was verified during each trial using a Spectronics Corporation Spectroline XS-254 UV-C photometer. After UV exposure, larvae were gently rinsed in a petri dish, collected, and placed in a vial containing approximately 1 ml of fly food. Vials were then stored in an incubator for 24 hours at 25°C before behavioral assay.

### Thermal nociception assay

Noxious stimuli were administered using a thermal probe (ProDev Engineering, Missouri City, Texas) by an operator blind to genotype and/or treatment. The thermal probe was set to deliver a temperature of 41°C, the highest innocuous temperature, to test for allodynia, or 45°C to assess normal nociception. Noxious thermal stimuli were administered along the dorsal midline between abdominal segments 2 and 5. Withdrawal behavior was defined as at least one 360° roll in response to the stimulus. Response latency was recorded, and responses were categorized as: under 6 seconds as fast, 6–20 seconds as slow and more than 20 seconds as no response.

### Quantification of dendritic morphology

In order to determine if observed changes in sensitivity of knockdown larvae are associated with changes in dendritic length and branching, class IV multidendritic neurons were measured for total dendritic length and dendritic branching. Third instar larvae measuring 4.5 to 4.9 mm in length were anesthetized with ether for 3 minutes then placed on a microscope slide in halocarbon-ether mixture (2:1). Using a Leica SP5 confocal microscope, nociceptors expressing ppk1.9-Gal4>UAS-mCD8-GFP were imaged between abdominal segments 4–6. Z stacks were taken using a 0.76 μm step size to capture the whole dendritic field. Images were taken at a size of 1024 × 1024. Using modifications previously described,<sup>34</sup> images were skeletonized and

analyzed for parameters of dendritic length and dendritic branching in the open-source image-processing package Fiji.<sup>35,36</sup>

### Localization of Schnurri GFP-tagged gene product

A PBac{shn-GFP.FBTB} line<sup>33</sup> (BDSC#42671) was used to visualize Schnurri via fusion with GFP (SHN::GFP), while ppk-CD4-tdTomato (BDSC#35844) allowed visualization of the nociceptor.

### Immunohistochemical analysis of Brinker expression

Third instar larvae expressing eGFP within their nociceptors (via ppk1.9-Gal4>UAS-mCD8-GFP), were filleted as previously described<sup>11</sup> and immediately fixed by 30-min incubation at room temperature (RT) with ice-cold 4% paraformaldehyde in phosphate buffered saline solution (PBS). Fixation was followed by washes in 1% PBT (1% Triton X-100 in PBS), which included two 1-min washes, one 10-min wash, and one 1-hr wash at RT. Washed fillets were then blocked using PBT-B (0.3% Triton X-100 + 1% bovine serum albumin (BSA) + PBS) for at least 1 hr at RT. After initial blocking, fillets were incubated overnight at 4°C using gentle rotation with guinea pig anti-BRK<sup>37</sup> at a dilution of 1:500 in PBT-B. Overnight incubation was followed by two 30-min washes in PBT-B with rotation and then a second blocking for 1 hr using fresh PBT-B + 5% normal goat serum (NGS) at RT. Following the second blocking, fillets were incubated for 2 hrs at RT with the fluorescently conjugated secondary antibody, goat anti-mouse AlexaFluor-647 (Catalog#: A-21236, Invitrogen, Thermo Fisher Scientific, Inc), diluted to 1:500 in PBT-B + 5% NGS. Fillets were then washed three times in 0.3% PBT (0.3% Triton X-100 in PBS) for 30-min, followed by two washes for 2 min with PBS. Fillets were mounted onto slides using Vectashield Antifade Mounting Medium with DAPI (H-1200, Vector Laboratories) for nuclear staining.

### Imaging and CTCF analysis

Nociceptors from third instar larvae fillets prepared for fluorescent analysis by immunohistochemistry were imaged with a Leica TCS SP5 confocal laser scanning microscope using a 40x oil objective and a HyD detector. Z-stacks were obtained with a 0.38 μm step size, a scan format of 1024 x 1024, and using uniform acquisition settings across experimental and control samples for smart gain, laser power, zoom, frame averaging, and pinhole. Using Fiji<sup>35,36</sup> five z-slices toward the mid-section of each nociceptor z-stack were sum projected and then cropped to remove the majority of dendritic structures and display the nociceptor soma primarily. Also, within Fiji, masks were made from these cropped sum

projections that corresponded to either the nucleus, visualized by DAPI fluorescence, or the soma, visualized by GFP fluorescence, to obtain regions of interest (ROIs) specific to that portion of the cell. Any overlapping nuclei (visualized by DAPI) surrounding the nociceptor was also masked and made into an ROI which was then cleared from each soma and nuclear mask before obtaining the final ROIs used for measurement, to account for any anti-BRK fluorescence that could arise from cells close to the nociceptor. Nuclear and soma ROIs were then used to measure area and integrated density in Fiji for anti-BRK fluorescence within the cropped sum projections and corrected total cellular fluorescence (CTCF) was calculated using the following calculation described previously.<sup>38</sup> CTCF equals integrated density minus (area of selected cells times mean fluorescence of background readings). The mean fluorescence of background was the average of three mean fluorescence measurements obtained using images of larval fillet controls that did not receive the primary antibody (anti-BRK). The CTCF for each sample/group was then averaged and a Student's *t* test was applied for statistical analysis in Microsoft Excel (version 2104). The same CTCF method was used for quantifying SHN::GFP fluorescence in the nociceptor, however, three background measurements for GFP signal were taken from three ppk1.9-CD4-tdTomato control samples (instead of no primary control samples) imaged in the same session as the experimental samples and using the same confocal settings.

### Statistical analysis

Mixed Logistic Regression (MLR) was performed to determine the predicted probability of reacting between different treatment groups in thermal probe behavioral assays. The response variable (reaction time) was compared to the explanatory variable (genotype, UV treatment) by generating a linear model and running MLR utilizing the program R.<sup>39</sup> In bar graphs depicting allodynia and normal nociception experiments, black boxes denote fast responders (<6 seconds), gray boxes denote slow responders (6–20 seconds), and white boxes denote non-responders (>20 seconds). Whiskers indicate the standard error of the mean of at least three groups of larvae. On graphs: \* =  $p < 0.05$ , \*\* =  $p < 0.01$ , \*\*\* =  $p < 0.001$ .

## Results

Since Brk represses BMP-regulated transcription, and the BMP pathway is known to regulate injury-induced behavioral sensitization,<sup>11</sup> we assessed whether nociceptor-specific knockdown of Brk would result in nociceptive hypersensitivity in the absence of injury. We used inverted repeat element Brk<sup>1R-1</sup> driven by the

nociceptor-specific *ppk-Gal4* driver to reduce *Brk* expression specifically in the nociceptor via RNA interference and verified the success of the knockdown by immunohistochemical analysis. Using an anti-BRK antibody<sup>37</sup> to detect protein in fixed tissues, we observed *Brk* expression in the nociceptors, and a significant reduction in immunofluorescent signal in the nuclei of *Brk-KD* nociceptors, compared to normal controls (Figure 2).

The nocifensive responses of *Brk* knockdown (*Brk-KD*) animals were then compared with controls. Uninjured *Brk-KD* animals were significantly more responsive to an innocuous thermal stimulus (41°C) compared to both controls (Figure 3(a)) and therefore can be said to exhibit genetically-induced thermal allodynia. Another experiment was conducted using a second, nonoverlapping *Brk* inverted repeat line (*Brk<sup>IR-2</sup>*). Results validated initial findings, showing significant response of uninjured animals to a normally innocuous thermal stimulus (41°C), (Figure 3(b)). The sensitivity of injured larvae in which *Brk* was knocked down was not significantly different from that of uninjured *Brk*-knockdown larvae (not shown). Furthermore, uninjured *Brk* knockdown larvae were significantly

more sensitive to a noxious thermal stimulus (45°C) than both controls, indicative of thermal hyperalgesia (Figure 3(c)).

We tested the possibility that nociceptors of larvae with altered BMP pathway activity also have altered morphology. To establish whether the observed changes in thermal nociceptive sensitivity were associated with an alteration of dendritic branching and/or dendritic length, nociceptors of *Brk-KD* and control animals were imaged using confocal microscopy in live animals expressing GFP in nociceptors using *ppk-eGFP*. Analysis detected no significant difference between the dendritic morphology of flies of control genotypes and those in which *Brk* was knocked down (Figure 2).

*Brk* repression is known to be relieved by the activator protein *Shn*.<sup>26,27</sup> To determine that this transcriptional regulation system is present in the nociceptor, we used a line in which a GFP tag had been inserted in the C-terminus of the *Shn* reading frame using the P [acman] system.<sup>33</sup> The *Shn* tagged GFP line was crossed with a line expressing *tdTomato* under the control of the pickpocket promoter in the nociceptors and progeny were imaged using confocal microscopy. CTCF analysis for determining signal over background revealed

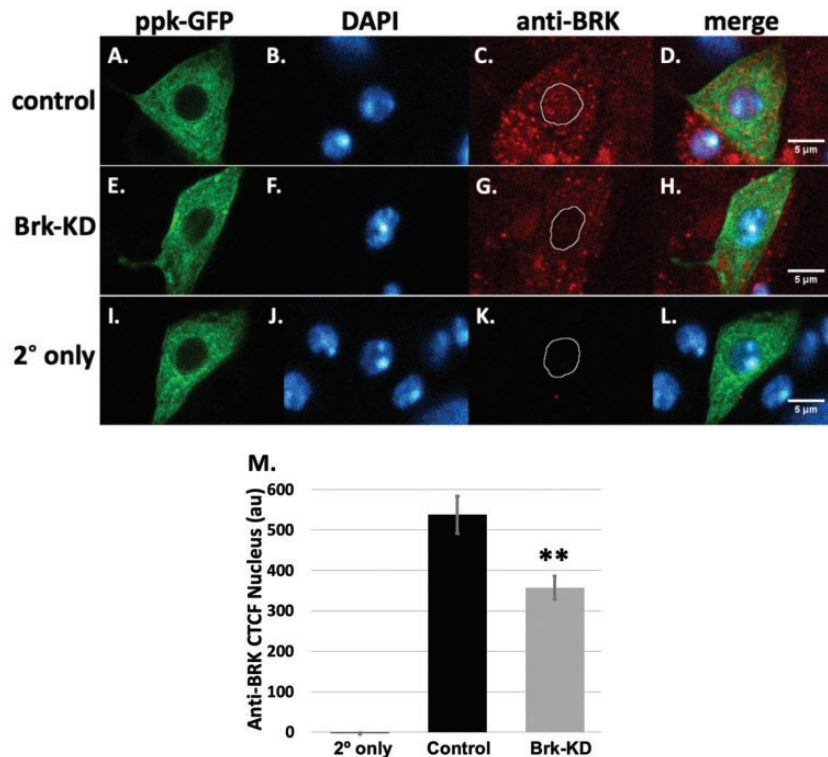


**Figure 2.** Immunofluorescent visualization of Brinker protein (BRK) in *Drosophila* larval nociceptors in control and *ppk1.9Gal4>UAS-Brk<sup>IR-1</sup>* animals. Nociceptors were visualized via *ppk1.9-Gal4>UAS-mCD8- GFP* (a, d, e, h, i, and l), nuclei via DAPI (b, d, f, h, j, and l), and BRK via anti-BRK primary antibody<sup>37</sup> and AlexaFluor 647-linked secondary (c, d, g, h, k, and l). White outlines in c, g, and k represent nociceptor nuclear area, generated by a DAPI-staining mask in Fiji. Significant reduction in BRK immunoreactivity (via CTCF method) was observed in nociceptor nuclei (c, g, k, and m). \*\* represents  $p < 0.01$ , Student's t-test.

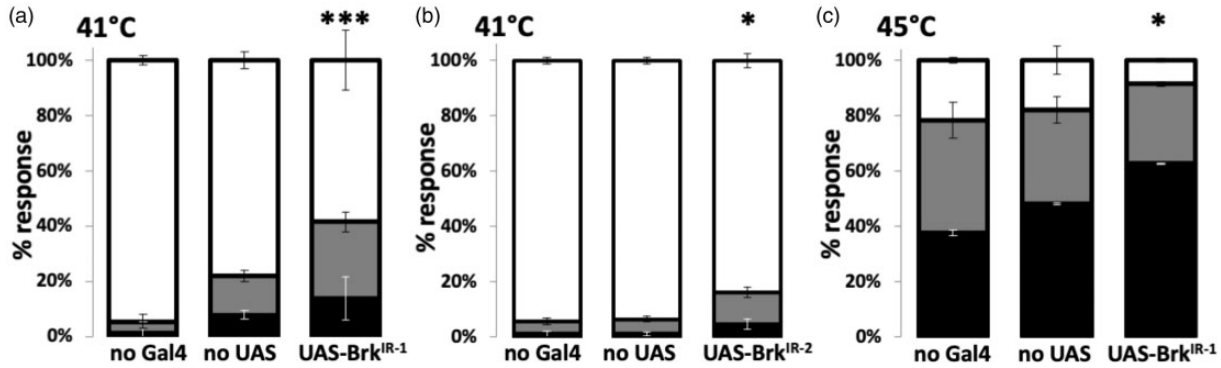


**Figure 3.** Knockdown of the repressor Brinker in nociceptors is sufficient for the formation of allodynia and hyperalgesia in uninjured animals. (a) Knockdown of Brinker using  $ppk1.9-Gal4 > UAS$ -inverted repeat  $Brk^{IR-1}$  resulted in genetically-induced allodynia in the absence of injury, compared to both controls, as shown by reaction to normally subthreshold temperature of 41 °C. (b) A second experiment conducted using  $ppk1.9-Gal4$  and a non-overlapping Brk UAS-inverted repeat,  $Brk^{IR-2}$  showed less-pronounced but similar results. (c) Genetically induced hyperalgesia was demonstrated using a normally noxious temperature of 45 °C.  $N = 90$  for all groups. Response latencies were classified as follows: none (>20 s, white), slow (between 6 s and 20 s, gray) and fast (<6 s, black). Whiskers indicate Standard error of the mean (SEM) of at least three groups of larvae ( $N = 90-121$ ). \*\*\* represents  $p < 0.001$ , \* represents  $p < 0.05$ , analyzed via Fisher's Exact test.

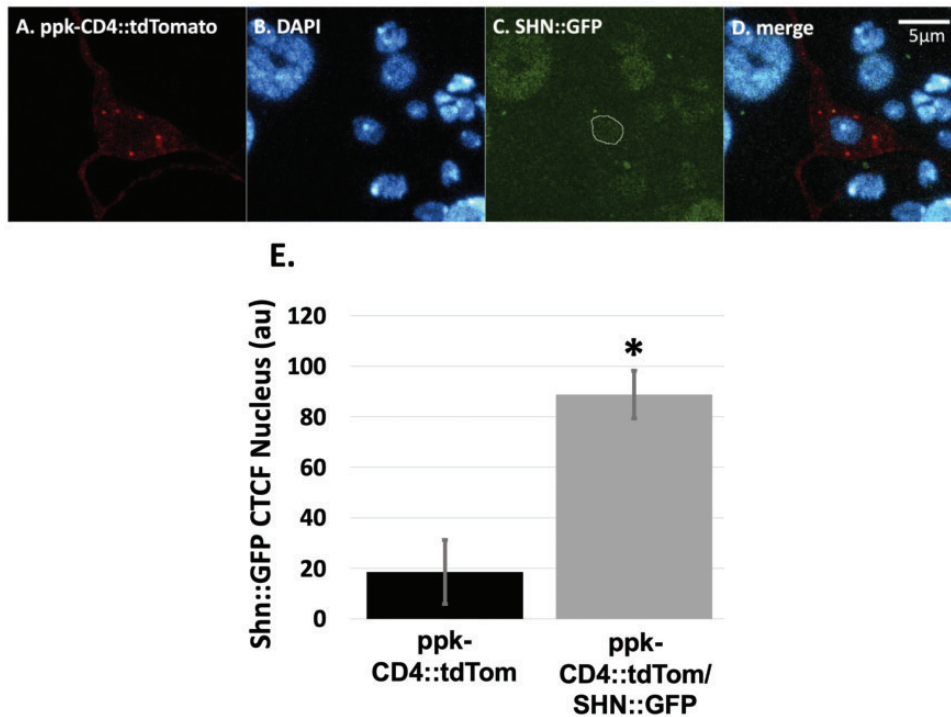


**Figure 4.** Transcriptional regulator Schnurri is expressed in the nociceptor. Schnurri ( $SHN::GFP^{33}$ ) expression in nociceptor was confirmed by colocalization using  $ppk-CD4$ - $tdTomato$  expression in the nociceptor (red: a and d), DAPI indicating nuclei (blue: b and d) and  $SHN::GFP$  (green: c and d). White outline in c represents nociceptor nuclear area, generated by a DAPI-staining mask in Fiji. CTCF analysis comparing  $SHN::GFP$  fluorescence to background in  $tdTomato$  controls revealed  $SHN::GFP$  in the nuclei of nociceptors (e), and signal is also apparent in nociceptor somata, as well as in other unidentified cells (merge: d).  $N = 3$  per group, \* represents  $p < 0.05$ , Student's t-test.

localization of Shn within the nociceptor (Figure 4). Nociceptors in Brk-knockdown larvae showed no significant difference in either dendritic branching or total dendritic length (Figure 6).

Since both Shn (Figure 4) and Brk (Figure 2) are expressed in the nociceptor, it might be predicted that knockdown of Shn would result not in hypersensitivity in uninjured animals, but in an inability to sensitize after

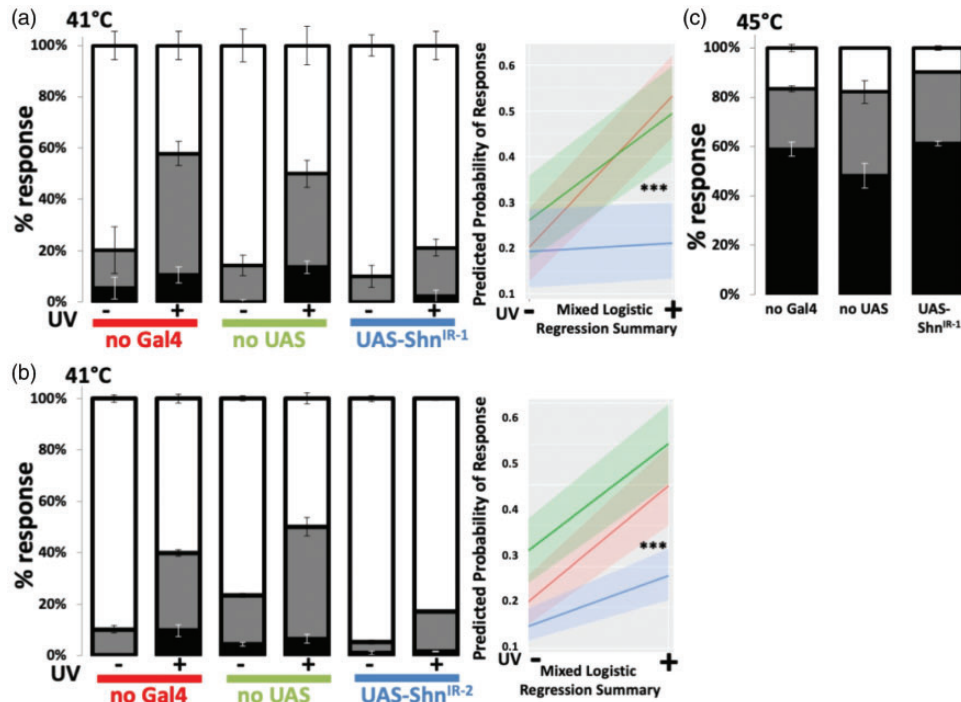


**Figure 5.** The transcriptional activator Schnurri (Shn) is required by the nociceptor for injury-induced allodynia. Knockdown of Shn using *ppk1.9-Gal4>Shn* UAS-inverted repeat (a) *Shn*<sup>IR-1</sup> or (b) *Shn*<sup>IR-2</sup> resulted in a failure to produce allodynia after injury, compared to both controls. Larvae were treated with either mock injury (–) or UV-injury (+), and then assayed with a thermal probe set to 41°C, 24 hours later. (c). Suppression of Shn in nociceptors does not alter sensitivity in the absence of injury. Normal nociception was assessed with a probe set to a normally noxious temperature of 45°C. Uninjured animals with Shn knocked down in nociceptors using *ppk1.9-Gal4>UAS*-inverted repeat *Shn*<sup>IR-1</sup> were not different from either control. Responses were classified as follows: none (>20 s, white), slow (between 6 s and 20 s, gray) and fast (<6 s, black). Whiskers indicate standard error of the mean (SEM) of at least three groups of larvae (N = 90–111). Results were analyzed by mixed logistic regression. \*\*\* indicates  $p < 0.001$ .

injury. This hypothesis was tested by stimulating injured *Shn* knockdown larvae at the highest innocuous temperature, 41°C. Knockdown of *Shn* expression using either *Shn*<sup>IR-1</sup> (Figure 5(a)) or non-overlapping *Shn*<sup>IR-2</sup> (Figure 5(b)) driven by the nociceptor-specific *ppk-Gal4* driver resulted in larvae that were unable to produce injury-induced thermal allodynia, compared to both controls. To test whether this observed blockade of injury induced allodynia was the result of a general hyposensitivity to thermal stimuli, uninjured *Shn* knockdown larvae were also tested at the normally noxious 45°C, but no significant differences from controls were observed (Figure 5 (c)).

In order to establish whether the observed changes in thermal nociceptive sensitivity in larvae with *Shn* knocked down were associated with an alteration of dendritic branching and/or dendritic length, nociceptors of live *Shn*-suppressed and control animals were imaged using confocal microscopy expressing GFP in nociceptors using *ppk-eGFP*. Analysis detected no significant difference between the dendritic branching of flies of control genotypes and those in which *Shn* was knocked down, however did detect a significant reduction in

overall dendritic length (Figure 6). This suggests that the hypersensitivity observed in *Shn* knockdown genotypes may be, at least in part, a product of morphological changes produced by knockdown of *Shn*.

## Discussion

Our findings indicate transcription regulators of the Dpp signaling pathway that are necessary for the control of nociceptive sensitivity. Previous studies have implicated other components of other upstream signaling pathways including *Tk*<sup>10</sup> and *Hh*<sup>9</sup> in the formation of nociceptor sensitization. Furthermore, epistasis studies have suggested that these pathways act in sequence and regulate the sensitization phenomenon through the TRP channels *Painless* and *dTRPA1*.<sup>8</sup> Here, we show evidence of another level of complexity to this response, indicating that the nociceptive sensitization in class IV multidendritic sensory neurons, referred to here as nociceptors, acts through nuclear mechanisms to regulate downstream transcriptional targets.

The *Brk* transcriptional repressor system downstream of Dpp's receptors and canonical intracellular

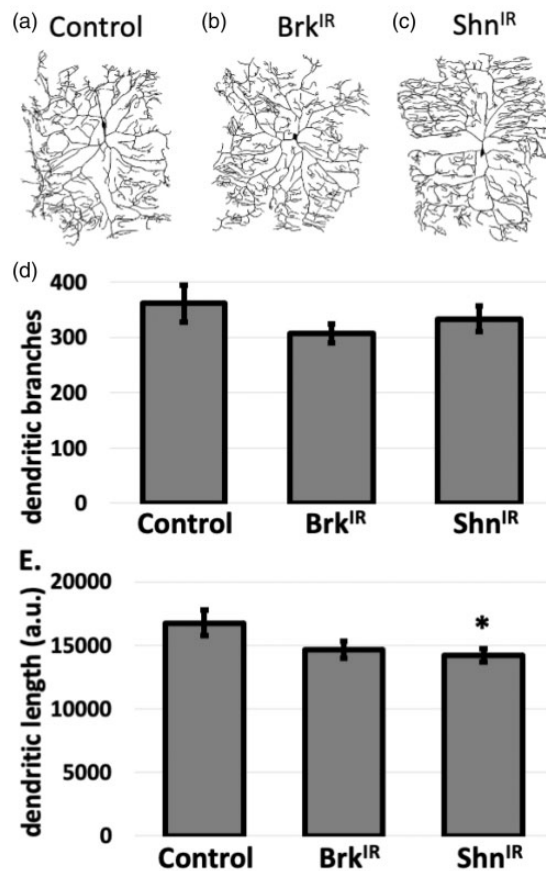


**Figure 6.** Analysis of morphology of dendritic fields in nociceptors which Brinker (Brk) or Schnurri (Shn) is knocked down. Morphology of nociceptor dendritic fields was visualized in control (a: *ppk1.9Gal4>y<sup>1</sup>v<sup>1</sup>*), Brk-knockdown (b: *ppk1.9Gal4>UAS-Brk<sup>IR-1</sup>*), and Shn-knockdown larvae (c: *ppk1.9Gal4>UAS-Shn<sup>IR-1</sup>*). Images represent live nociceptors expressing GFP via UAS-mCD8::GFP (a–c). Dendritic branching (d) and length (e) were not significantly different in Brk-knockdown nociceptors. Dendritic length (e) but not branching (d) was reduced in Shn-knockdown nociceptors compared to control. Neuronal dendritic branching (d) and length (e) were assessed using a Fiji image-processing package. Data were analyzed by Welch's t-test,  $n = 9$  per experimental group. \* indicates  $p < 0.05$ .

transducers is perhaps one of the best studied of all such complexes in nature. Before now, the Brk repressor had not been implicated in the formation of nociceptive sensitization, and had only been minimally studied in the nervous system.<sup>26</sup> In order to investigate the mechanisms underlying nociceptive sensitization, we used the GAL4/UAS system to study this phenomenon in a tissue specific manner. The nociceptors, which extensively tile the inner surface of the *Drosophila* larval integument, are responsible for the avoidance response to noxious thermal and mechanical stimuli.<sup>40</sup> Nociceptors express nociceptive ion channels such as Pickpocket (Ppk), a DEG/ENaC channel necessary for the response to noxious

mechanical stimuli,<sup>31,32</sup> *Drosophila* Transient Receptor Potential A1 (dTRPA1) that senses thermal stimuli, and Painless (pain), a Transient Receptor Potential channel that detects both thermal and mechanical stimuli.<sup>8</sup> Previous experiments have established that activity of dTRPA1 and pain are modulated by injury,<sup>9,11</sup> but the connection to BMP signaling has yet to be detailed. This study adds to the knowledge of how transcriptional regulation controlled by BMP signaling leads to hypersensitivity.

After epidermal injury by ultraviolet light, cytokines are released from the epidermis onto underlying nociceptors<sup>9</sup> and presumably trigger Dpp release, which then binds its receptors on the nociceptors.<sup>11</sup> Dpp's intracellular transducer molecules Mad and Med then enter the nucleus and there interact with Brk and Shn, with the effect of relieving repression by Brk,<sup>26,27</sup> effectively releasing the pathways's target genes for transcription.

When Brk expression was knocked down in nociceptors (Figure 2), we observed hypersensitivity in the absence of injury, indicating that even in the absence of canonical Dpp signaling or tissue damage, removal of Brk's repression can cause allodynia and hyperalgesia phenotypes (Figure 3(a) and (b)). The observed hypersensitivity phenotype of Brk knockdown, coupled with our previous observations of the hyposensitivity resulting from Dpp knockdown,<sup>11</sup> reflect the antagonistic relationship between Brk and Dpp, which is already known to determine expression limits during development.<sup>41,42</sup> Nociceptor-specific knockdown of Brk was not associated with any detectable changes in dendritic morphology (Figure 6), suggesting that the observed hypersensitivity is not due to a morphogenetic effect.

When Shn, also expressed in the nociceptor (Figure 4), was knocked down in the nociceptor, we observed a failure to produce injury-induced allodynia (Figure 5(a) and (b)). This manipulation produced no significant changes to nociceptor dendritic branching, but a significant reduction in dendritic length (Figure 6). These results suggest that Shn is necessary to promote nociceptor hypersensitivity after injury, and that Shn may play a morphogenetic role in the nociceptor. Some inter-experiment differences in the responses of controls are noted (compare Figures 3 and 5), a known factor in this assay,<sup>5,11</sup> which can be attributed to slight variation in operator technique.

The use of the UV injury model to investigate genetic involvement of the BMP signaling pathway in nociceptor sensitization represents significant clinical promise and a deeper understanding of this signaling process in nociceptors. This study implicates the nuclear steps of the BMP pathway in controlling nociceptor sensitivity, indicating a range of new targets for potential



pharmaceutical agents that could be used in the prevention and treatment of chronic pain.

Until this point, medicine has largely taken a reactive, rather than a proactive or preventative approach to chronic pain. Our current treatments, despite being effective in the short term, have failed millions of individuals and society as a whole globally due to both their lack of long-term effectiveness and their detrimental side effect profiles. This data reveals the potential for developing more targeted approaches to chronic pain management, including considerations for identifying populations at risk for the development of chronic pain states, and the delivery of treatments that prevent the occurrence of this condition. Novel targets described here modulate nociceptive sensitivity of the peripheral nociceptors themselves, and their topical pharmacological manipulation may obviate the need for systemic opioid medications.

### Acknowledgements

Stocks obtained from the Bloomington *Drosophila* Stock Center (NIH P40OD018537), including those generated by the TRiP at Harvard Medical School (NIH/NIGMS R01-GM084947), were used in this study. The ppk1.9-Gal4>UAS-mCD8-GFP line was a generous gift from Michael Galko, and the anti-BRK antibody was gifted to us by Aurelio Teleman.

### Declaration of Conflicting Interests

The author(s) declared no potential conflicts of interest with respect to the research, authorship, and/or publication of this article.

### Funding

The author(s) disclosed receipt of the following financial support for the research, authorship, and/or publication of this article: The authors received the support of NIH/NIGMS COBRE award 1P20GM103643-01A1 to I. Meng, the UNE Microscope Core Facility, funded by NSF Grants #0116398 and #1125672, NIH/NINDS award 2R15NS095195-02 to G. Ganter, and the technical support of Rema Weston and Michael Esty. Histology support was provided by the UNE COBRE Histology and Imaging Core.

### ORCID iD

Geoffrey Ganter  <https://orcid.org/0000-0001-7726-2111>

### References

- Dahlhamer J, Lucas J, Zelaya C, Nahin R, Mackey S, DeBar L, Kerns R, Von Korff M, Porter L, Helmick C. Prevalence of chronic pain and high-impact chronic pain among adults – United States, 2016. *MMWR Morb Mortal Wkly Rep* 2018; 67: 1001–1006.
- Goldberg DS, McGee SJ. Pain as a global public health priority. *BMC Public Health* 2011; 11: 770–770.
- Centers for Disease Control and Prevention. *Annual surveillance report of drug-related risks and outcomes – United States (Surveillance Special Report 2pdf icon)*. Washington, DC: Centers for Disease Control and Prevention, U.S. Department of Health and Human Services, 2018.
- Wide-Ranging Online Data for Epidemiologic Research. Atlanta, GA: CDC, National Center for Health Statistics, 2020.
- Babcock DT, Landry C, Galko MJ. Cytokine signaling mediates UV-induced nociceptive sensitization in *Drosophila* larvae. *Curr Biol* 2009; 19: 799–806.
- Viswanath V, Story GM, Peier AM, Petrus MJ, Lee VM, Hwang SW, Patapoutian A, Jegla T. Opposite thermosensor in fruitfly and mouse. *Nature* 2003; 423: 822–823.
- Xu SY, Cang CL, Liu XF, Peng YQ, Ye YZ, Zhao ZQ, Guo AK. Thermal nociception in adult *Drosophila*: behavioral characterization and the role of the painless gene. *Genes Brain Behav* 2006; 5: 602–613.
- Tracey WD Jr, Wilson RI, Laurent G, Benzer S. Painless, a *Drosophila* gene essential for nociception. *Cell* 2003; 113: 261–273.
- Babcock DT, Shi S, Jo J, Shaw M, Gutstein HB, Galko MJ. Hedgehog signaling regulates nociceptive sensitization. *Curr Biol* 2011; 21: 1525–1533.
- Im SH, Takle K, Jo J, Babcock D, Ma Z, Xiang Y, Galko M. Tachykinin acts upstream of autocrine hedgehog signaling during nociceptive sensitization in *Drosophila*. *eLife* 2015; 4: e10735.
- Follansbee TL, Gjelsvik KJ, Brann CL, McParland A, Longhurst C, Galko M, Ganter G. *Drosophila* nociceptive sensitization requires BMP signaling via the canonical SMAD pathway. *J Neurosci* 2017; 37: 8524–8533.
- Gjelsvik KJ, Follansbee TL, Ganter GK. Bone morphogenetic protein glass bottom boat (BMP5/6/7/8) and its receptor wishful thinking (BMPRII) are required for injury-induced allodynia in *Drosophila*. *Mol Pain* 2018; 14: 1744806918802703.
- Brann CL, Moulton JK, Ganter GK. Glypicans dally and dally-like control injury-induced allodynia in *Drosophila*. *Mol Pain* 2019; 15: 1744806919856777–1744806919856777.
- Affolter M, Basler K. The decapentaplegic morphogen gradient: from pattern formation to growth regulation. *Nat Rev Genet* 2007; 8: 663–674.
- O'Connor MB, Umulis D, Othmer HG, Blair SS. Shaping BMP morphogen gradients in the *Drosophila* embryo and pupal wing. *Development* 2006; 133: 183–193.
- Ramel M-C, Hill CS. Spatial regulation of BMP activity. *FEBS Lett* 2012; 586: 1929–1941.
- Raftery LA, Umulis DM. Regulation of BMP activity and range in *Drosophila* wing development. *Curr Opin Cell Biol* 2012; 24: 158–165.
- Ashe HL. BMP signalling: synergy and feedback create a step gradient. *Curr Biol* 2005; 15: R375–377.
- Shrivage BV, Altmann G, Technau M, Roth S. The role of dpp and its inhibitors during eggshell patterning in *Drosophila*. *Development* 2007; 134: 2261–2271.
- Yakoby N, Lembong J, Schüpbach T, Shvartsman SY. *Drosophila* eggshell is patterned by sequential action of

- feedforward and feedback loops. *Development* 2008; 135: 343–351.
21. Ozkaynak E, Rueger DC, Drier EA, Corbett C, Ridge RJ, Sampath TK, Oppermann H. OP-1 cDNA encodes an osteogenic protein in the TGF-beta family. *EMBO J* 1990; 9: 2085–2093.
  22. Jones CM, Lyons KM, Hogan BL. Involvement of bone morphogenetic protein-4 (BMP-4) and vgr-1 in morphogenesis and neurogenesis in the mouse. *Development* 1991; 111: 531–542.
  23. Chen Y, Riese MJ, Killinger MA, Hoffmann FA. Genetic screen for modifiers of *Drosophila* decapentaplegic signaling identifies mutations in punt, mothers against dpp and the BMP-7 homologue, 60A. *Development* 1998; 125: 1759–1768.
  24. Campbell G, Tomlinson A. Transducing the dpp morphogen gradient in the wing of *Drosophila*: regulation of dpp targets by brinker. *Cell* 1999; 96: 553–562.
  25. Jaźwińska A, Rushlow C, Roth S. The role of brinker in mediating the graded response to dpp in early *Drosophila* embryos. *Development* 1999; 126: 3323–3334.
  26. Gafner L, Dalessi S, Escher E, Pyrowolakis G, Bergmann S, Basler K. Manipulating the sensitivity of signal-induced repression: quantification and consequences of altered brinker gradients. *PLoS One* 2013; 8: e71224–e71224.
  27. Chayengia M, Veikkolainen V, Jevtic M, Pyrowolakis G. Sequence environment of BMP-dependent activating elements controls transcriptional responses to dpp signaling in *Drosophila*. *Development* 2019; 146: dev176107.
  28. Maekawa T, Sakura H, Sudo T, Ishii S. Putative metal finger structure of the human immunodeficiency virus type 1 enhancer binding protein HIV-EP1. *J Biol Chem* 1989; 264: 14591–14593.
  29. Sampath TK, Rashka KE, Doctor JS, Tucker RF, Hoffmann FM. *Drosophila* transforming growth factor beta superfamily proteins induce endochondral bone formation in mammals. *Proc Natl Acad Sci U S A* 1993; 90: 6004–6008.
  30. Padgett RW, Wozney JM, Gelbart WM. Human BMP sequences can confer normal dorsal-ventral patterning in the *Drosophila* embryo. *Proc Natl Acad Sci U S A* 1993; 90: 2905–2909.
  31. Adams CM, Anderson MG, Motto DG, Price MP, Johnson WA, Welsh MJ. Ripped pocket and pickpocket, novel *Drosophila* DEG/ENaC subunits expressed in early development and in mechanosensory neurons. *J Cell Biol* 1998; 140: 143–152.
  32. Ainsley JA, Pettus JM, Bosenko D, Gerstein CE, Zinkevich N, Anderson MG, Adams CM, Welsh MJ, Johnson WA. Enhanced locomotion caused by loss of the *Drosophila* DEG/ENaC protein Pickpocket1. *Curr Biol* 2003; 13: 1557–1563.
  33. Kudron MM, Victorsen A, Gevirtzman L, Hillier LW, Fisher WW, Vafeados D, Kirkey M, Hammonds AS, Gersch J, Ammouri H, Wall ML, Moran J, Steffen D, Szynekarek M, Seabrook-Sturgis S, Jameel N, Kadaba M, Patton J, Terrell R, Corson M, Durham TJ, Park S, Samanta S, Han M, Xu J, Yan K-K, Celniker SE, White KP, Ma L, Gerstein M, Reinke V, Waterston RH. The ModERN resource: genome-wide binding profiles for hundreds of *Drosophila* and *Caenorhabditis elegans* transcription factors. *Genetics* 2018; 208: 937–949.
  34. Iyer EP, Iyer SC, Sullivan L, Wang D, Meduri R, Graybeal LL, Cox DN. Functional genomic analyses of two morphologically distinct classes of *Drosophila* sensory neurons: post-mitotic roles of transcription factors in dendritic patterning. *PLoS One* 2013; 8: e72434.
  35. Schindelin J, Arganda-Carreras I, Frise E, Kaynig V, Longair M, Pietzsch T, Preibisch S, Rueden C, Saalfeld S, Schmid B, Tinevez J-Y, White DJ, Hartenstein V, Eliceiri K, Tomancak P, Cardona A. Fiji: an open-source platform for biological-image analysis. *Nat Methods* 2012; 9: 676–682.
  36. Arganda-Carreras I, Fernández-González R, Muñoz-Barrutia A, Ortiz-De-Solorzano C. 3D reconstruction of histological sections: application to mammary gland tissue. *Microsc Res Tech* 2010; 73: 1019–1029.
  37. Doumpas N, Ruiz -Romero M, Blanco E, Edgar B, Corominas M, Teleman AA. Brk regulates wing disc growth in part via repression of myc expression. *EMBO Rep* 2013; 14: 261–268.
  38. McCloy RA, Rogers S, Caldon CE, Lorca T, Castro A, Burgess A. Partial inhibition of Cdk1 in G2 phase overrides the SAC and decouples mitotic events. *Cell Cycle* 2014; 13: 1400–1412.
  39. R Core Team. *R: a language and environment for statistical computing*. Vienna: R Foundation for Statistical Computing, 2020.
  40. Grueber WB, Jan LY, Jan YN. Tiling of the *Drosophila* epidermis by multidendritic sensory neurons. *Development* 2002; 129: 2867–2878.
  41. Minami M, Kinoshita N, Kamoshida Y, Tanimoto H, Tabata T. Brinker is a target of dpp in *Drosophila* that negatively regulates dpp-dependent genes. *Nature* 1999; 398: 242–246.
  42. Jaźwińska A, Kirov N, Wieschaus E, Roth S, Rushlow C. The *Drosophila* gene brinker reveals a novel mechanism of dpp target gene regulation. *Cell* 1999 ; 96: 563–573.